A Raman spectroscopic study of uranyl minerals from Cornwall, UK

R J P Driscoll,[a] D Wolverson,[*a] J M Mitchels,[a] J M Skelton,[a] S C Parker,[a] M Molinari,[a] I Khan,[b] D Geeson,[b] and G C Allen[c]

Received Xth XXXXXXXXXX 20XX, Accepted Xth XXXXXXXXX 20XX
First published on the web Xth XXXXXXXXXX 200X
DOI: 10.1039/b000000x

SUPPORTING INFORMATION

[a] *University of Bath, Claverton Down, Bath, UK.*
[*] Fax: XX XXXX XXXX; Tel: XX XXXX XXXX; E-mail: D.Wolverson@bath.ac.uk
[b] *AWE, Aldermaston, Reading, UK.*
[c] *Interface Analysis Center, University of Bristol, Bristol, UK.*

1 Physical appearance of the uranyl mineral samples

Autunite from Merrivale Quarry appears as fine, yellow crystals on a white, grey and black background rock, approximately 6 cm in diameter.

Torbernite from Bunny Mine appeared as small (approximately 600 μm across), green, tabular crystals on a grey and brown primary rock, approximately 11 cm in diameter.

Nováčekite from Wheal Edward was present as yellow and green flakes on a black and brown primary rock, approximately 5 cm across.

Zeunerite from Wheal Gorland appeared as fine green crystals on a light brown background rock, approximately 7 cm across.

Phosphuranylite from Wheal Edward occurred as a yellow crust on a brown rock (approximately 7 cm across), with fine, green associated crystals.

Andersonite and schröckingerite, both from Geevor Mine, are present as yellow mineral deposits on a brown background rock (both around 4 cm across); both samples have a thin layer of transparent gypsum crystals associated with the uranyl mineral.

Johannite from Geevor Mine is present as pale green crystals on a yellow-brown background rock, approximately 5 cm across.

Natrozippeite mineral from Geevor Mine occurs as a yellow crust on a black and brown primary rock (about 7 cm across); it is associated with small, green crystals that do not contain a uranyl cation.

Uranophane from Wheal Edward is present as a pale yellow crust on a light brown primary rock sample (approximately 7 cm across); it is associated with a black vein of pitchblende.

Kasolite from Loe Warren Zawn occurs as an orange-red crust on one face of a large grey primary rock sample, approximately 12 cm across.

Compreignacite and cuprosklodowskite were present as dark yellow and green crystals, respectively, on the same sample of brown, black and grey rock from West Wheal Owles.

2 Raman peak tables and wavelength comparisons

The tables shown in this section detail the vibrational bands seen in the Raman spectra for each mineral in this investigation. The positions given are an average of the same band seen in multiple spectra of the same sample, and both the standard deviation and the number of spectra in which each peak is seen are given. Literature bands are given; these have typically been deconvoluted. The assignment is based upon that given for the published spectra. The figures shown here illustrate the Raman spectra collected using all three excitation wavelengths for each mineral.

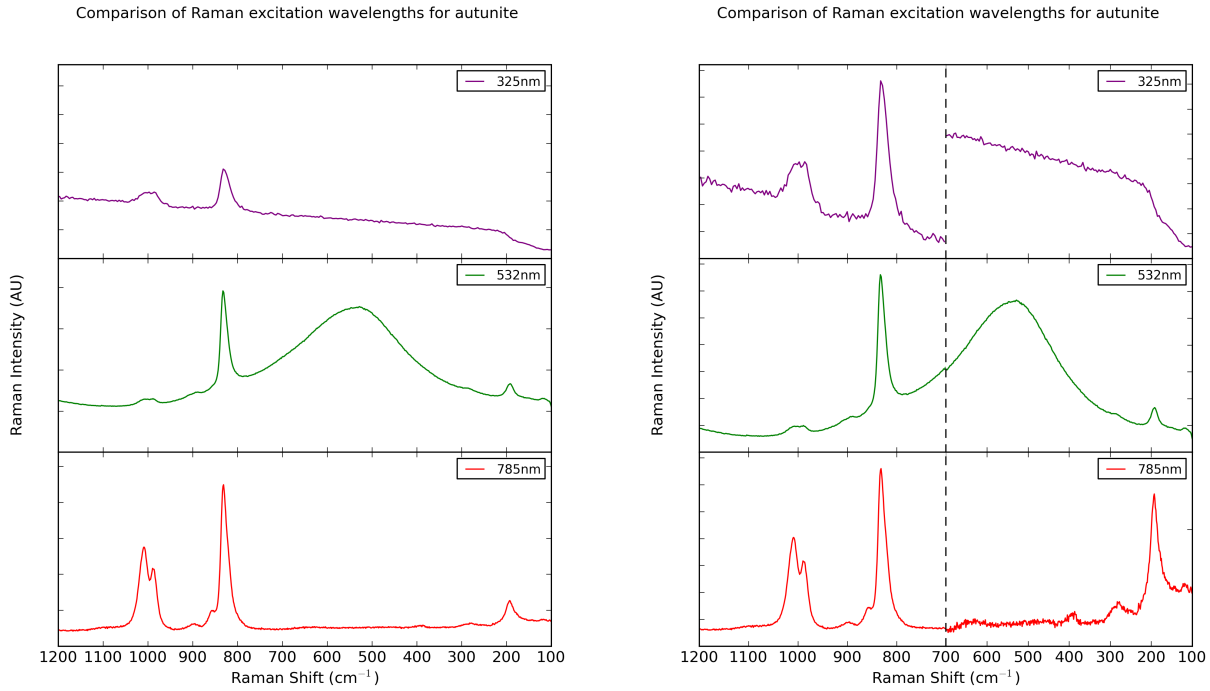

Fig. SI 1 A comparison of the three laser wavelengths for the uranyl phosphate mineral autunite. The left figure shows the raw spectra. Each section of the spectra shown on the right have been rescaled, separately, to emphasise the bands.

Table SI 1 Raman spectral bands for the uranyl phosphate mineral autunite

This Study			Literature[2]	
Position (cm^{-1})	Standard Deviation	Number of spectra	Position (cm^{-1})	Attribution
193 †	1.7	31	190, 222	Lattice Vibrations
283 *	4.2	19	291	$v_2(UO_2)^{2+}$ bend
–	–	–	399, 406, 439, 464	$v_2(PO_4)^{3-}$ bend
–	–	–	629	$v_4(PO_4)^{3-}$ bend
830	3.6	60	816, 822, 833	$v_1(UO_2)^{2+}$ symm. stretch
899 *	4.93	9	–	$v_3(UO_2)^{2+}$ antisymm. stretch
990	2.67	21	988	
1001 §	7.53	31	1007	$v_3(PO_4)^{3-}$ symm. stretch
1008	4.16	21	1018	

Sixty individual spectra were analysed for this sample of autunite.
* Low intensity or broad bands, not always visible in spectra.
† The 193 cm^{-1} peak was most prominent within the 785 nm spectra.
§ The 1001 cm^{-1} peak was only visible when the 990 and 1008 cm^{-1} peaks were not.

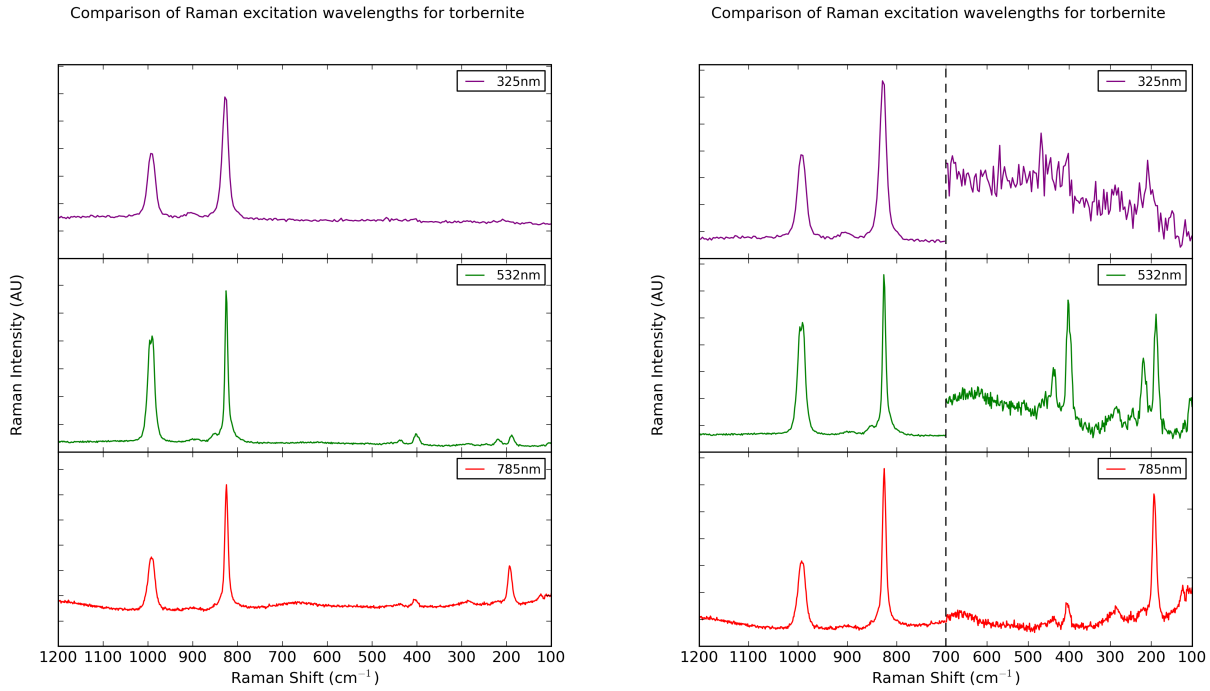

Fig. SI 2 A comparison of the three laser wavelengths for the uranyl phosphate mineral torbernite. The left figure shows the raw spectra. Each section of the spectra shown on the right have been rescaled, separately, to emphasise the bands.

Table SI 2 Raman spectral bands for the uranyl phosphate mineral torbernite

This Study			Literature[2]	
Position (cm^{-1})	Standard Deviation	Number of spectra	Position (cm^{-1})	Attribution
191 *	2.3	26	–	Lattice Vibrations
–	–	–	222, 290	$v_2(UO_2)^{2+}$ bend
404 *	2.7	24	399, 406, 439, 464	$v_2(PO_4)^{3-}$ bend
440 *	3.9	9		
–	–	–	629	$v_4(PO_4)^{3-}$ bend
825	1.8	38	808, 826	$v_1(UO_2)^{2+}$ symm. stretch
903 *	2.1	10	900	$v_3(UO_2)^{2+}$ antisymm. stretch
992	1.75	38	957, 988, 995, 1004	$v_3(PO_4)^{3-}$ antisymm. stretch

Thirty eight individual spectra were analysed for this sample of torbernite.
* Low intensity or broad bands, not always visible in spectra.

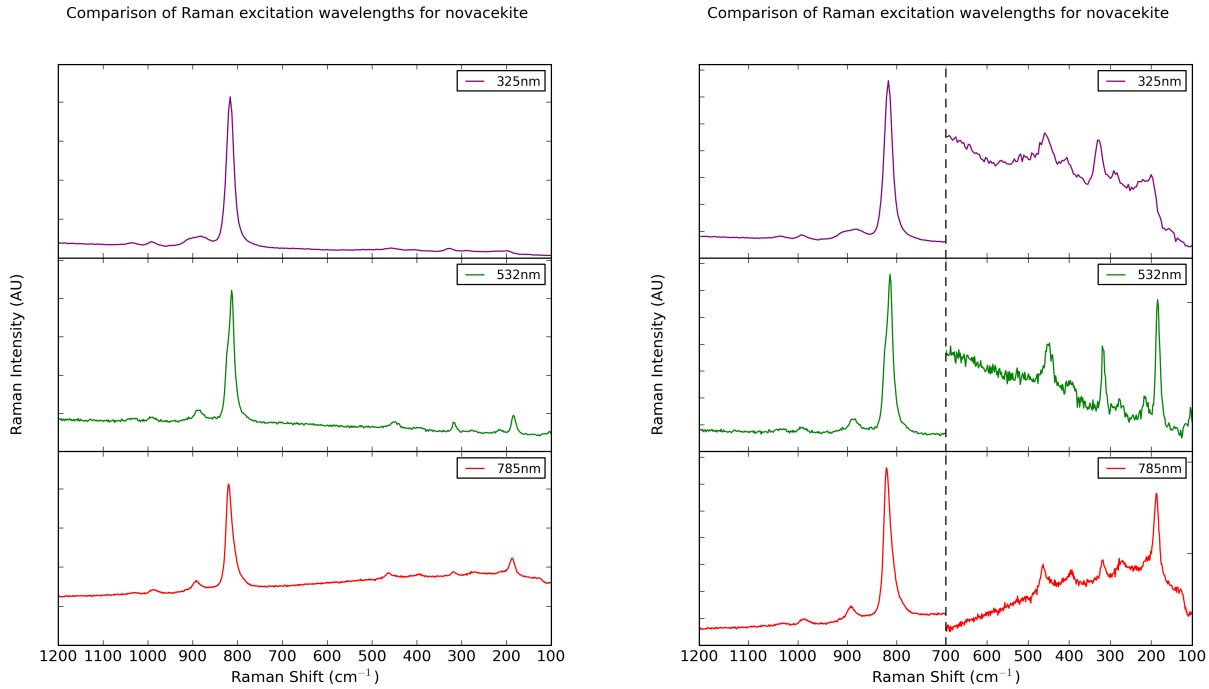

Fig. SI 3 A comparison of the three laser wavelengths for the uranyl arsenate mineral novacekite. The left figure shows the raw spectra. Each section of the spectra shown on the right have been rescaled, separately, to emphasise the bands.

Table SI 3 Raman spectral bands for the uranyl arsenate mineral nováčekite

Position (cm^{-1})	This Study Standard Deviation	Number of spectra	Literature [10] Saléeite Peak Positions (cm^{-1})	Literature [2]	Attribution
185	2.9	28	177, 196	–	Lattice Vibrations
269 *	6.0	10	218, 234, 283	284	$v_2(UO_2)^{2+}$ bend
325 *	4.3	14			$v_2(PO_4)^{3-}$ bend
452 *	2.6	10	376, 405, 446, 471	389	or
471 *	5.5	8			$v_2(AsO_4)^{3-}$ bend
–	–	–	573, 612	643	$v_4(PO_4)^{3-}$ bend
817	2.6	55	827, 843	818, 833, 847	$v_1(UO_2)^{2+}$ symm. stretch
889	5.6	36	896	–	$v_3(UO_2)^{2+}$ antisymm. stretch
989	2.3	11	980, 994, 1007	982, 988, 1007	$v_3(PO_4)^{3-}$ antisymm. stretch
1034 *	2.6	7			

Fifty five individual spectra were analysed for this sample of nováčekite.
No literature spectra are available for a direct comparison with nováčekite, so its spectrum has been compared against saléeite, its phosphate analogue.
* Low intensity or broad bands, not always visible in spectra.

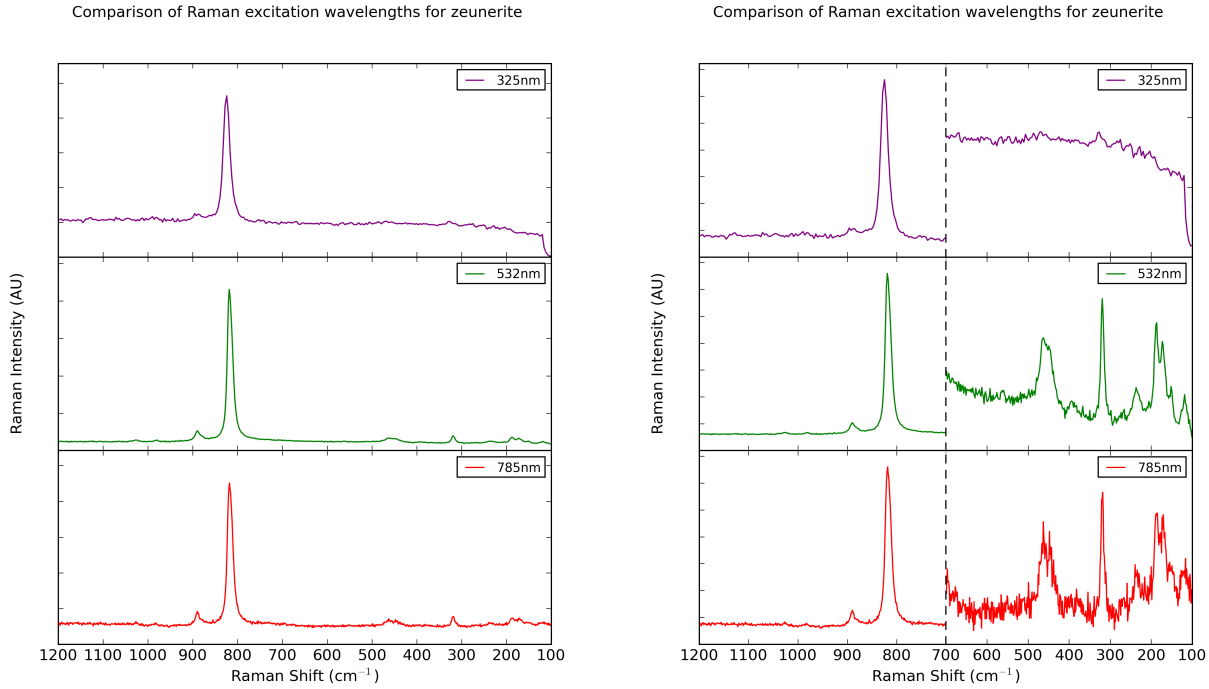

Fig. SI 4 A comparison of the three laser wavelengths for the uranyl arsenate mineral zeunerite. The left figure shows the raw spectra. Each section of the spectra shown on the right have been rescaled, separately, to emphasise the bands.

Table SI 4 Raman spectral bands for the uranyl arsenate mineral zeunerite

Position (cm^{-1})	This Study Standard Deviation	Number of spectra	Literature[11] Position (cm^{-1})	Attribution
–	–	–	182	Lattice Vibrations
–	–	–	218, 235, 275	$v_2(UO_2)^{2+}$ bend
323 *	4.9	5	320, 380	$v_2(AsO_4)^{3-}$ bend
404 *	4.6	7	396	$v_4(AsO_4)^{3-}$ bend
463	6.6	19	446, 463	
821	3.0	25	811, 818	$v_1(UO_2)^{2+}$ symm. stretch
886	4.5	16	890	$v_3(UO_2)^{2+}$ antisymm. stretch
987	1.7	9	–	unknown
1029 *	2.8	4	–	unknown

Twenty five individual spectra were analysed for this sample of zeunerite.
* Low intensity or broad bands, not always visible in spectra.

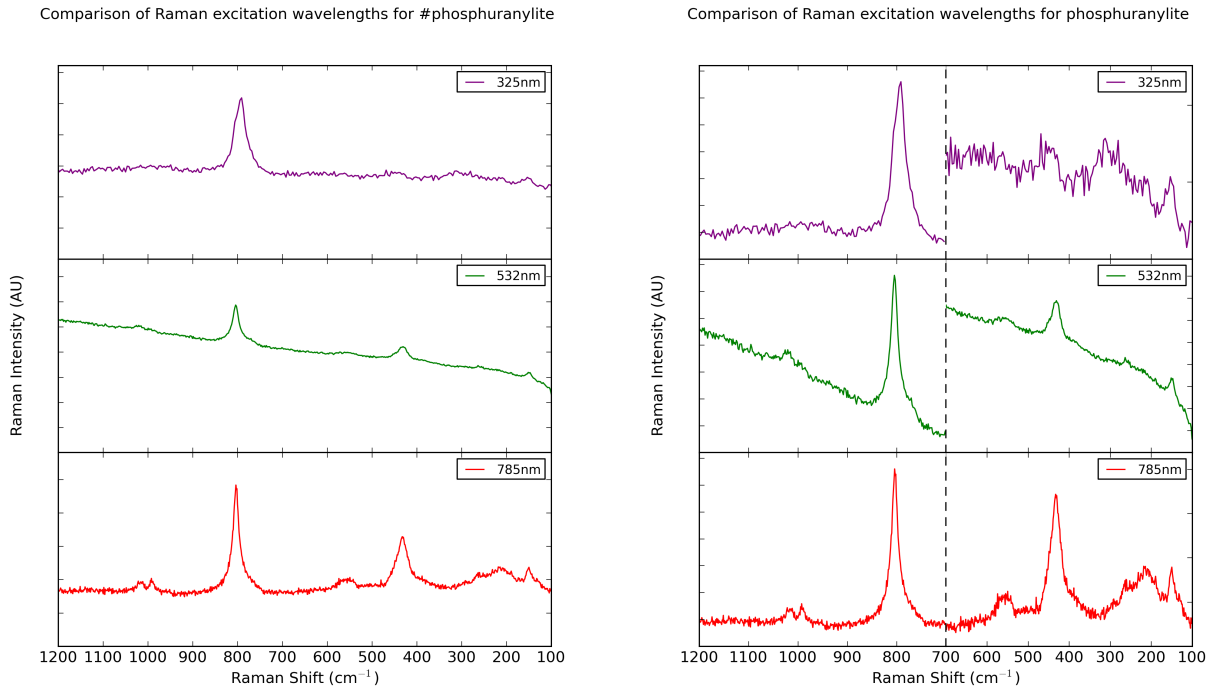

Fig. SI 5 A comparison of the three laser wavelengths for the uranyl phosphate mineral phosphuranylite. The left figure shows the raw spectra. Each section of the spectra shown on the right have been rescaled, separately, to emphasise the bands.

Table SI 5 Raman spectral bands for the uranyl phosphate mineral phosphuranylite

This Study			Literature[4]			
Position (cm^{-1})	Standard Deviation	Number of spectra	Minerva Heights	Saddle Ridge Position (cm^{-1})	Ruggles Mine	Attribution
148 *	2.3	16	111, 152, 175	117, 145, 166	112, 147, 161	Lattice Vibrations
216 *	4.2	13	211	205	208	$v_2(UO_2)^{2+}$ bend
239 *	3.7	5	220	227, 240	238	
260 *	3.9	13	263	267	267	
283 *	3.4	5	295	294	287	
312 *	5.3	6				
435	6.0	25	404, 435, 452	368, 394, 417, 439	396, 398, 421, 437, 452, 476	$v_2(PO_4)^{3-}$ bend
558 *	2.7	7	564, 613, 655	500, 532, 566	511, 515, 536, 569, 616	$v_4(PO_4)^{3-}$ bend
801	4.9	29	768, 793, 805, 815	816, 837, 843, 847	812, 817, 832, 841	$v_1(UO_2)^{2+}$ symm. stretch
–	–	–	–	–	894	$v_3(UO_2)^{2+}$ antisymm. stretch
992 †	2.8	10	992	1009	1005	$v_3(PO_4)^{3-}$ antisymm. stretch
1017 †	1.2	8	1016	1050	1032, 1050, 1055	
–	–	–	1122	1125	1124	

Twenty nine individual spectra were analysed for this sample of phosphuranylite.
* Low intensity or broad bands, not always visible in spectra.
† The 992 and 1017 cm^{-1} bands appear together, in a small number of 785 nm spectra.

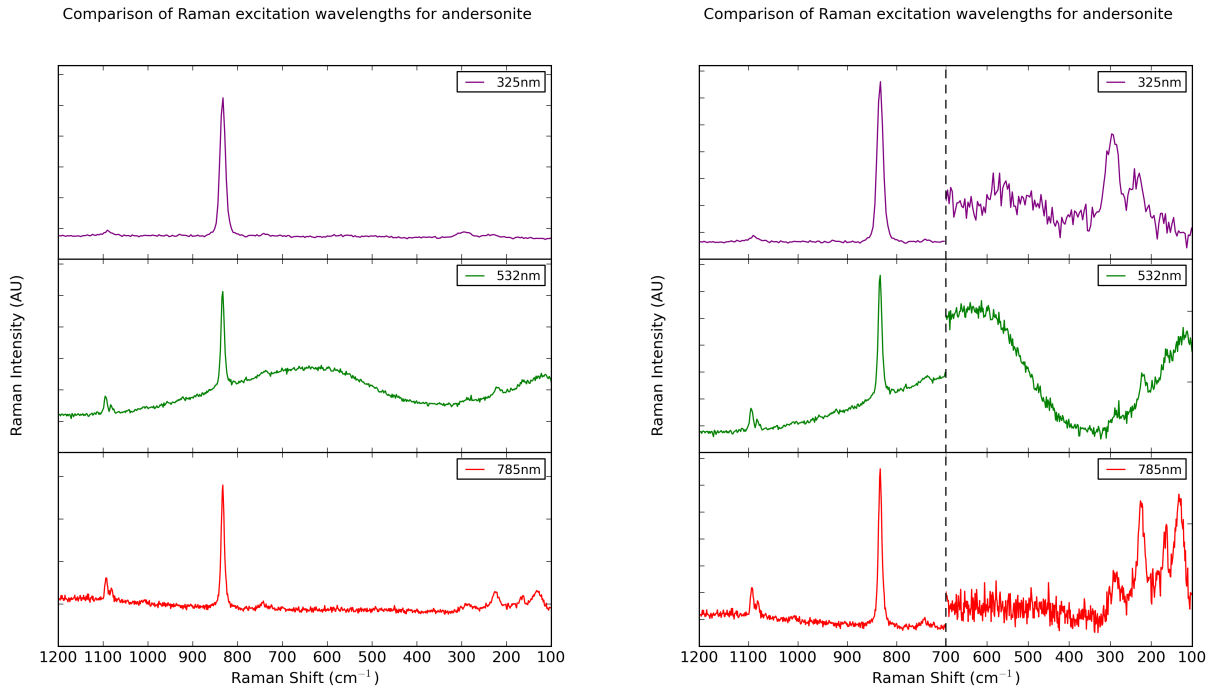

Fig. SI 6 A comparison of the three laser wavelengths for the uranyl carbonate mineral andersonite. The left figure shows the raw spectra. Each section of the spectra shown on the right have been rescaled, separately, to emphasise the bands.

Table SI 6 Raman spectral bands for the uranyl carbonate mineral andersonite

This Study			Literature[3]	
Position (cm^{-1})	Standard Deviation	Number of spectra	Position (cm^{-1})	Attribution
130	3.1	7	164, 182	Lattice Vibrations
225 *	5.2	8	224, 242, 284, 299	$v_2(UO_2)^{2+}$ bend
291 *	3.3	6		
743 *	2.0	4	697, 732, 744	$v_4(CO_3)^{2-}$ bend
833	0.5	15	830, 833	$v_1(UO_2)^{2+}$ symm. stretch
1092	2.3	15	1080, 1092	$v_1(CO_3)^{2-}$ symm. stretch
–	–	–	1370, 1406	$v_3(CO_3)^{2-}$ antisymm. stretch

Fifteen individual spectra were analysed for this sample of andersonite.
* Low intensity or broad bands, not always visible in spectra.

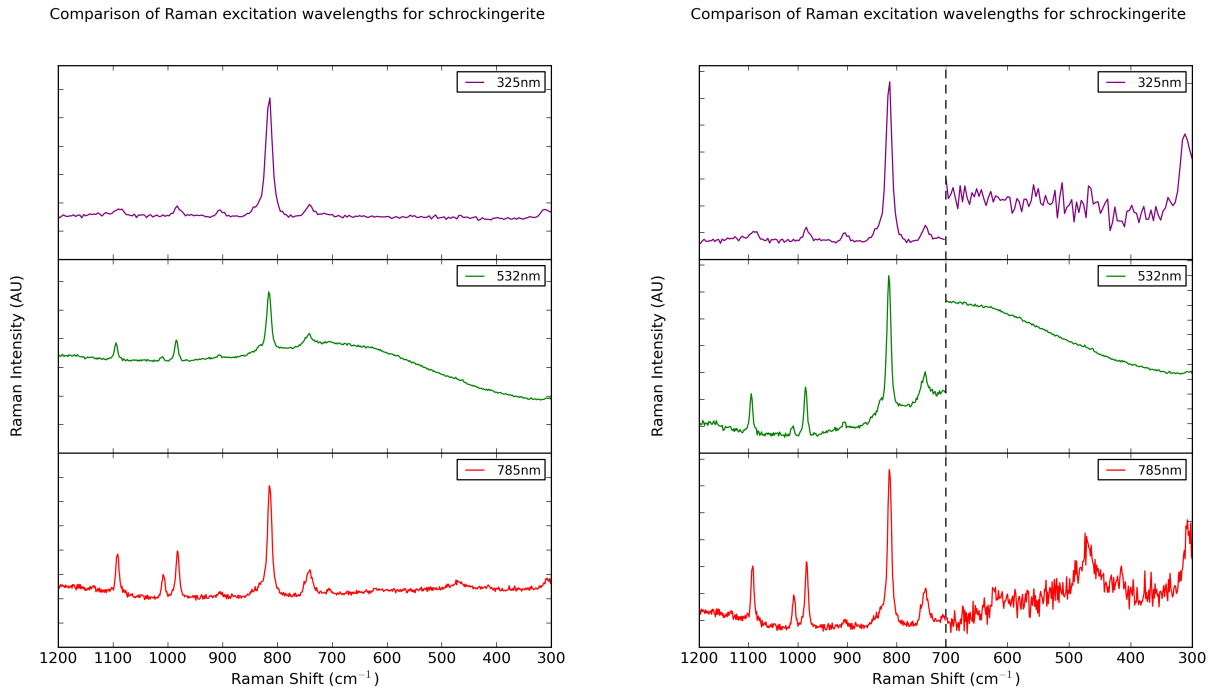

Fig. SI 7 A comparison of the three laser wavelengths for the uranyl carbonate mineral schröckingerite. The left figure shows the raw spectra. Each section of the spectra shown on the right have been rescaled, separately, to emphasise the bands.

Table SI 7 Raman spectral bands for the uranyl carbonate mineral schröckingerite

This Study			Literature[6]	
Position (cm^{-1})	Standard Deviation	Number of spectra	Position (cm^{-1})	Attribution
–	–	–	157	Lattice Vibrations
253 *	0.5	3	308	$v_2(UO_2)^{2+}$ bend
307 *	2.9	4		
416 *	3.8	5	471	$v_2(SO_4)^{2-}$ bend
496 *	3.6	6		
743	2.1	16	707, 742	$v_4(CO_3)^{2-}$ bend
815	1.0	21	815	$v_1(UO_2)^{2+}$ symm. stretch
984	2.0	14	983	$v_1(SO_4)^{2-}$ symm. stretch
1009 *	0.8	12		
1093	1.8	12	1092	$v_1(CO_3)^{2-}$ symm. stretch
1136	3.3	9	1090, 1100, 1147	$v_3(SO_4)^{2-}$ antisymm. stretch

Twenty one individual spectra were analysed for this sample of schröckingerite.
* Low intensity or broad bands, not always visible in spectra.

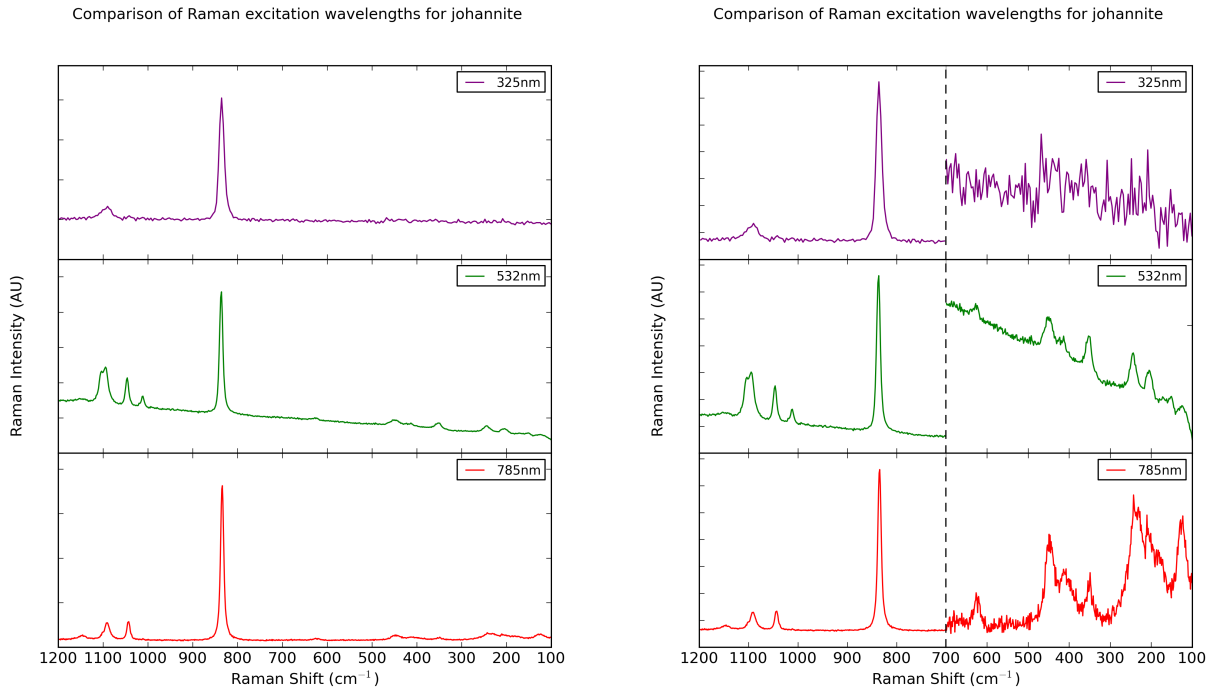

Fig. SI 8 A comparison of the three laser wavelengths for the uranyl sulphate mineral johannite. The left figure shows the raw spectra. Each section of the spectra shown on the right have been rescaled, separately, to emphasise the bands.

Table SI 8 Raman spectral bands for the uranyl sulphate mineral johannite

This Study Position (cm^{-1})	Standard Deviation	Number of spectra	Literature[9] Position (cm^{-1})	Attribution
–	–	–	184	Lattice Vibrations
203 *	3.0	13	205	$v_2(UO_2)^{2+}$ bend
244 *	2.4	10	277	
–	–	–	302	Cu-O stretch
352 *	0.8	6	384	$v_2(SO_4)^{2-}$ bend
448 *	1.7	7	481, 539	$v_4(SO_4)^{2-}$ bend
836	1.1	30	756, 788, 812	$v_1(UO_2)^{2+}$ symm. stretch
–	–	–	948, 975	$v_3(UO_2)^{2+}$ antisymm. stretch
1045	1.3	14	1042	$v_1(SO_4)^{2-}$ symm. stretch
1095	3.1	18	1009, 1100, 1147	$v_3(SO_4)^{2-}$ antisymm. stretch

Thirty individual spectra were analysed for this sample of johannite.
* Bands are only visible in a number of 532 and 785 nm spectra.

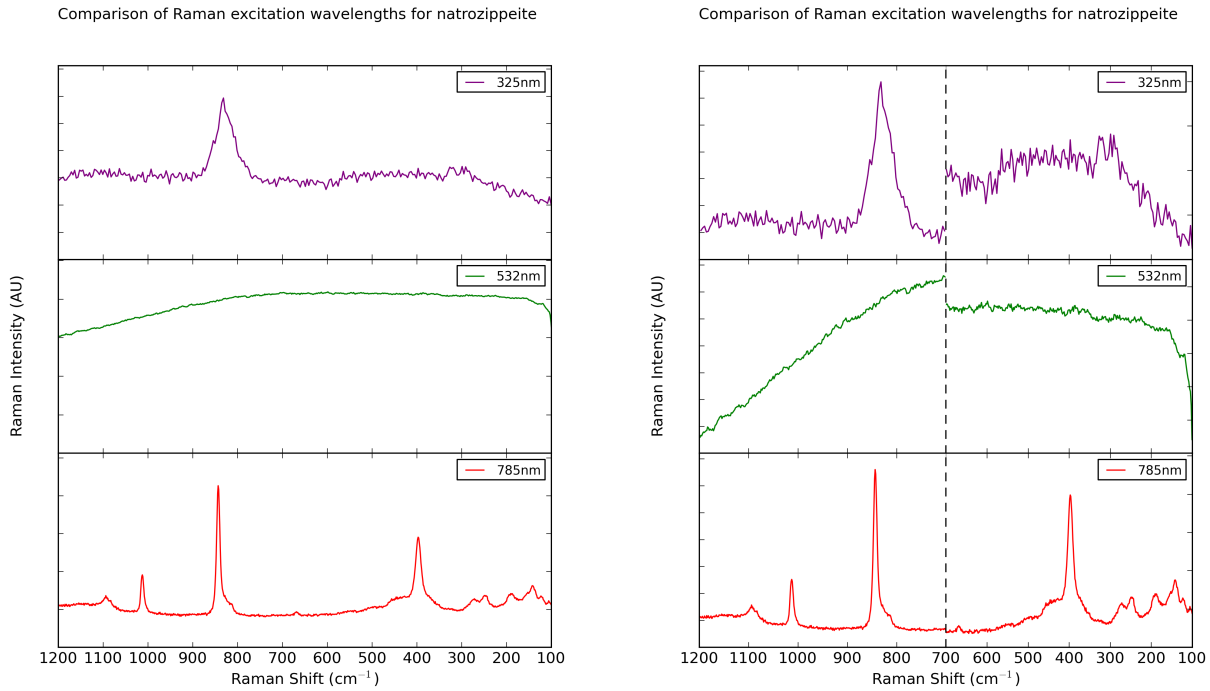

Fig. SI 9 A comparison of the three laser wavelengths for the uranyl sulphate mineral natrozippeite. The left figure shows the raw spectra. Each section of the spectra shown on the right have been rescaled, separately, to emphasise the bands.

Table SI 9 Raman spectral bands for the uranyl sulphate mineral natrozippeite

This Study			Literature[5]	
Position (cm^{-1})	Standard Deviation	Number of spectra	Position (cm^{-1})	Attribution
191 *	1.1	16	196	Lattice Vibrations
250 *	2.1	10	250	$v_2(UO_2)^{2+}$ bend
397	1.8	28	373, 398, 431, 498	$v_2(SO_4)^{2-}$ bend
–	–	–	669	$v_4(SO_4)^{2-}$ bend
840	4.5	38	813, 823, 834, 840, 841	$v_1(UO_2)^{2+}$ symm. stretch
1013	0.7	21	980, 1007, 1010	$v_1(SO_4)^{2-}$ symm. stretch
1094 *	1.5	15	1081, 1091, 1130	$v_3(SO_4)^{2-}$ antisymm. stretch
1159 *	4.1	12		

Thirty eight individual spectra were analysed for this sample of natrozippeite.
No information was forthcoming from the 532 nm spectra, as a fluorescence band drowned the region under investigation. The wavelength that gave the best spectra was 785 nm.
* Bands are not consistently visible in all spectra.

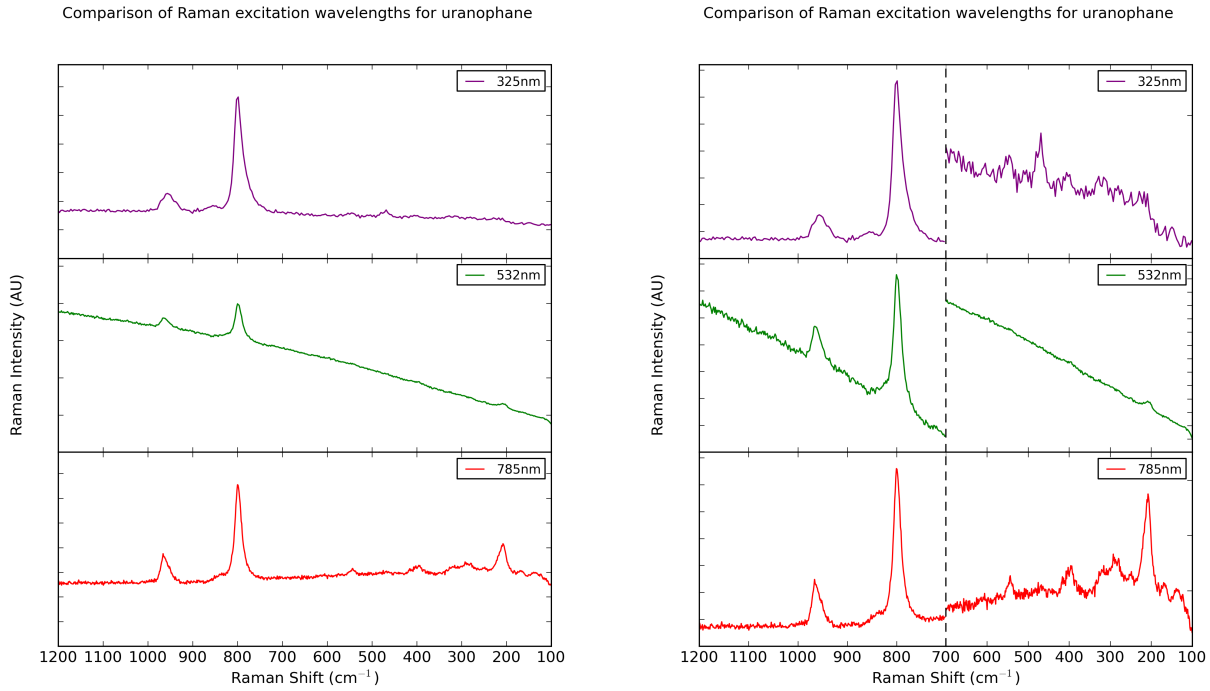

Fig. SI 10 A comparison of the three laser wavelengths for the uranyl silicate mineral uranophane. The left figure shows the raw spectra. Each section of the spectra shown on the right have been rescaled, separately, to emphasise the bands.

Table SI 10 Raman spectral bands for the uranyl silicate mineral uranophane

This Study			Literature [7]	
Position (cm^{-1})	Standard Deviation	Number of spectra	Position (cm^{-1})	Attribution
209 *	2.8	13	213, 250, 280, 288, 324	$v_2(UO_2)^{2+}$ bend
283 *	3.4	6		
399 *	2.0	6	398, 469	$v_2(SiO_4)^{4-}$ bend
544 *	0.9	6	544	$v_4(SiO_4)^{4-}$ bend
800	1.4	21	711, 786, 792, 796	$v_1(UO_2)^{2+}$ symm. stretch
856 *	1.7	3	–	$v_3(UO_2)^{2+}$ antisymm. stretch
961	3.5	16	960, 963	$v_3(SiO_4)^{4-}$ antisymm. stretch

Twenty one individual spectra were analysed for the sample of uranophane.
* Bands are not consistently visible in all spectra.

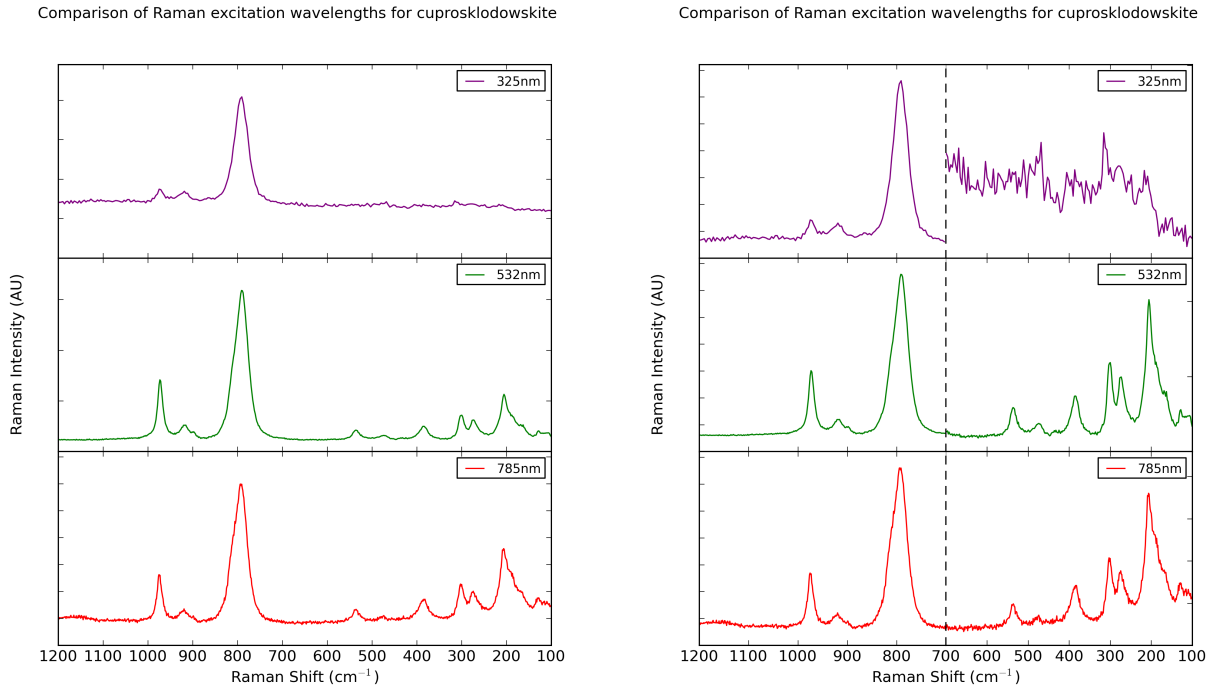

Fig. SI 11 A comparison of the three laser wavelengths for the uranyl silicate mineral cuprosklodowskite. The left figure shows the raw spectra. Each section of the spectra shown on the right have been rescaled, separately, to emphasise the bands.

Table SI 11 Raman spectral bands for the uranyl silicate mineral cuprosklodowskite

This Study			Literature [7]	
Position (cm^{-1})	Standard Deviation	Number of spectra	Position (cm^{-1})	Attribution
203	2.4	13	205, 217	$v_2(UO_2)^{2+}$ bend
273 *	3.1	5	267, 276	
299 *	1.0	5	301	
312 *	0.9	3		
384 *	0.5	3	411, 476	$v_2(SiO_4)^{4-}$ bend
–	–	–	507, 535	$v_4(SiO_4)^{4-}$ bend
792	1.6	19	746, 758, 774, 787	$v_1(UO_2)^{2+}$ symm. stretch
919 *	2.0	6	–	$v_3(UO_2)^{2+}$ antisymm. stretch
974	2.1	13	974	$v_3(SiO_4)^{4-}$ antisymm. stretch

Nineteen individual spectra were analysed for the sample of cuprosklodowskite.
* Bands are not consistently visible in all spectra.

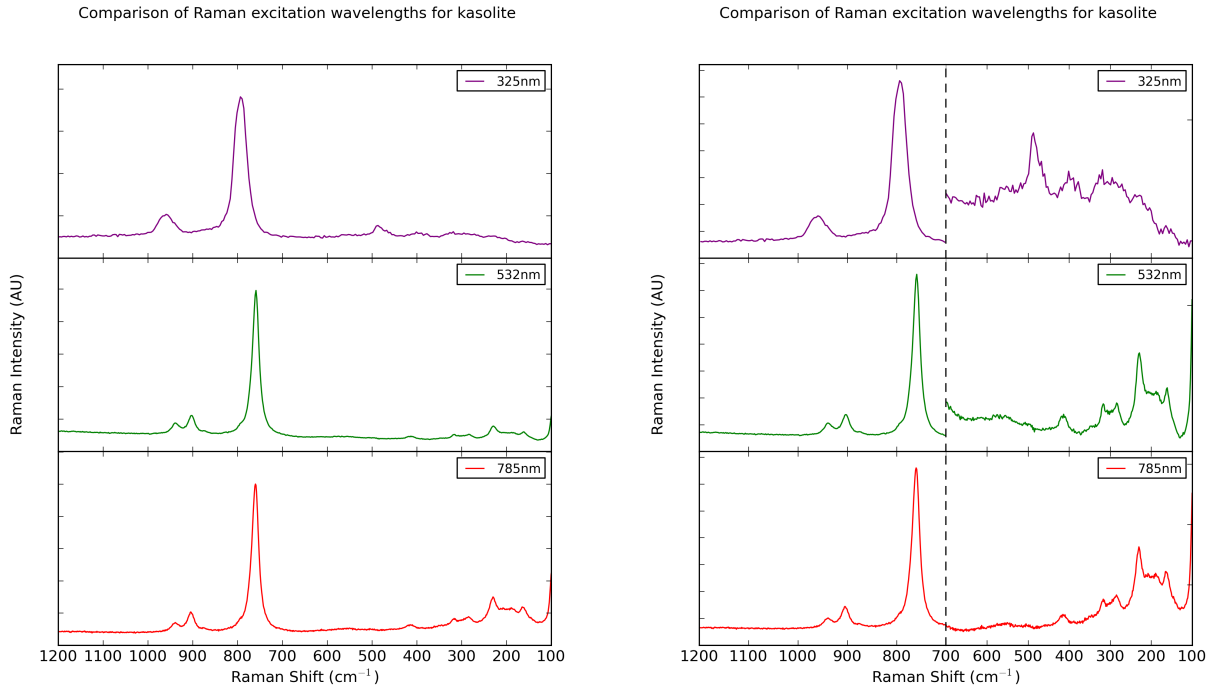

Fig. SI 12 A comparison of the three laser wavelengths for the uranyl silicate mineral kasolite. The left figure shows the raw spectra. Each section of the spectra shown on the right have been rescaled, separately, to emphasise the bands.

Table SI 12 Raman spectral bands for the uranyl silicate mineral kasolite

This Study			Literature [7]	
Position (cm^{-1})	Standard Deviation	Number of spectra	Position (cm^{-1})	Attribution
196	8.5	8	154, 165, 185	Lattice Vibrations
230	0.5	8	217, 231, 234, 285, 302	$v_2(UO_2)^{2+}$ bend
415 *	1.0	3	415, 454	$v_2(SiO_4)^{4-}$ bend
–	–	–	501, 533, 575	$v_4(SiO_4)^{4-}$ bend
760	0.5	9	721, 750, 758, 766, 793	$v_1(UO_2)^{2+}$ symm. stretch
904	0.9	8	903	$v_3(UO_2)^{2+}$ antisymm. stretch
939	0.9	6	–	$v_3(SiO_4)^{4-}$ antisymm. stretch

Nine individual spectra were analysed for this sample of kasolite.
* Bands are not consistently visible in all spectra.

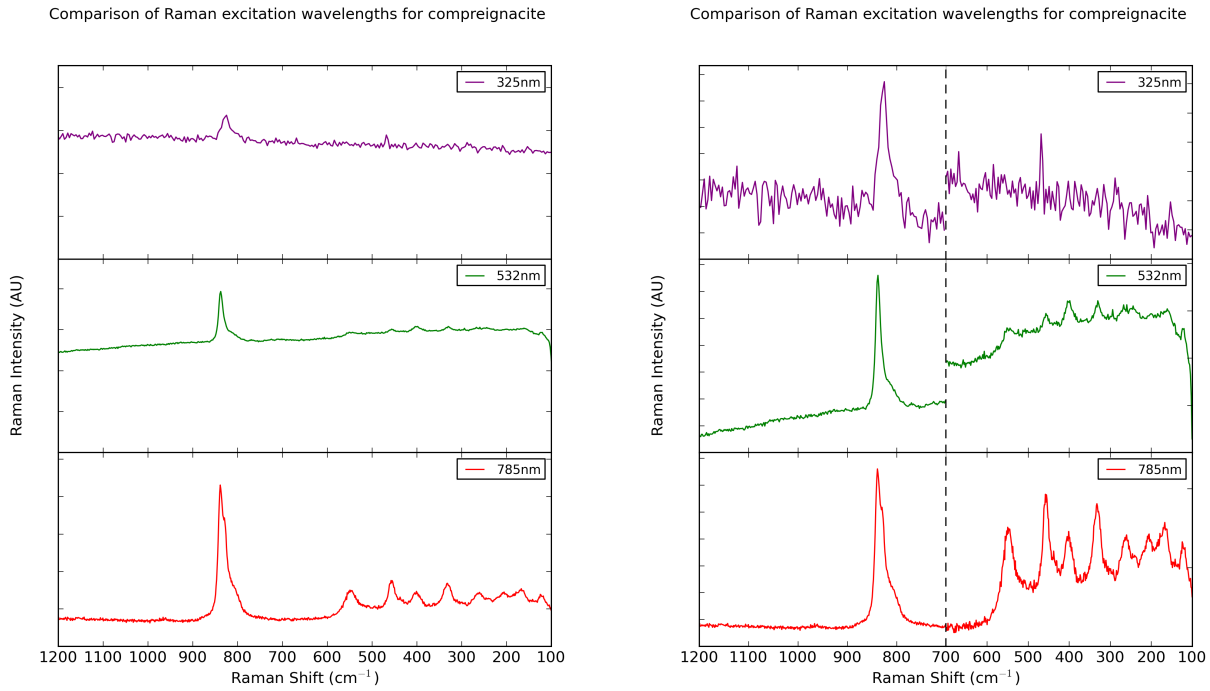

Fig. SI 13 A comparison of the three laser wavelengths for the uranyl hydrate mineral compreignacite. The left figure shows the raw spectra. Each section of the spectra shown on the right have been rescaled, separately, to emphasise the bands.

Table SI 13 Raman spectral bands for the uranyl silicate mineral compreignacite

This Study Position (cm^{-1})	Standard Deviation	Number of spectra	Literature[8] Position (cm^{-1})	Attribution
164 *	3.0	6	153	Lattice Vibrations
204 *	1.9	7	197, 253	$v_2(UO_2)^{2+}$ bend
329 *	5.3	10	–	unknown
402 *	3.7	8	439	$v(U_3O)$ stretch)
460 *	5.0	12	–	unknown
549	1.1	7	602, 687	U-O-H bend and water liberation
834 †	4.24	38	824, 848	$v_1(UO_2)^{2+}$ symm. stretch
–	–	–	1010, 1050, 1080, 1110, 1160, 1190, 1330, 1454	U-O-H bending

Thirty eight individual spectra were analysed for this sample of compreignacite.
* Bands are not consistently visible in all spectra.
† A smaller peak or shoulder is sometimes present about 804 cm^{-1} in 785 nm spectra, or about 858 cm^{-1} in 325 nm spectra.

3 Analysis of the EDX data

Table SI 14 The EDX analysis of the minerals in this investigation

Mineral Name	Atomic Percentage (±1%), averaged over multiple spectra												
	U	O	P	As	Si	S	Cu	Ca	Mg	Na	K	Pb	F
Autunite	7.5	81.1	5.9	0.8				3.7					
Torbernite	8.3	80.3	7.6	0.2			3.7						
Nováčekite	6.3	86.8	0.9	3.8					2.2				
Zeunerite	8.4	80.0	1.7	6.3			3.6						
Phosphuranylite	8.7	77.5	5.5	0.4				3.8			2.2		
Andersonite	3.2	74.4				4.1		9.6		3.2			5.5
Schröckingerite	4.9	69.5				4.1		13.7		2.6			5.1
Johannite	6.1	80.4			2.0	5.6	4.2						
Natrozippeite	12.2	77.1				5.6				5.1			
Uranophane	7.5	80.7			7.7			3.0					
Cuprosklodowskite	7.3	77.1	1.5	1.4	9.2		2.6						
Kasolite	7.1	76.4			7.0							6.8	
Compreignacite	12.1	80.7			1.9	3.0					2.3		

Carbon is not shown in the EDX, as the percentage is too high to reliably predict the mineral composition. This is likely due to the presence of carbon in the background rock and the carbon tape used to mount the sample.
The percentage values shown here only consider the elements present in significant quantites; any elements that were present below 1% have not been included in this table and may be considered as part of the background rock.
The concentration of uranium is typically slightly higher than expected from the ratio of polyanion, which may be explained by the presence of uranium in the background rock. The only difference to this is for the uranyl silicates, where the silicon ratio tends to be higher than the uranium. However, silicon was seen in trace quantities for almost all spectra, often alongside aluminium and other elements. Overall, the ratios of uranium to polyanion generally agree with literature values.
The layered structure seen in the majority of minerals allows for cations to move through the interlayer space, which may account for the cation ratio variation in different samples. A cation deficiency is seen in natrozippeite, uranophane, cuprosklodowskite and compreignacite.
The most significant deviation from theoretical composition are seen in the uranyl carbonate mineral andersonite. The theoretical formula has a 2:1 ratio of sodium:calcium, whereas the EDX seen here contains significantly more calcium, alongside the unexpected presence of sulphur and fluorine. These elements may be explained by the presence of gypsum ($CaSO_4$, reported by Elton and Hooper[1]) and perhaps fluorspar (CaF_2), which are both common components of gangue (the host-rock).

Table SI 15 Estimation of the chemical composition for the minerals in this investigation, based on the EDX spectra

Mineral	Theoretical Composition	Estimate from EDX
Autunite	$Ca(UO_2)_2(PO_4)_2{\cdot}11H_2O$	$Ca(UO_2)_2(PO_4)_{1.6}(AsO_4)_{0.2}$
Torbernite	$Cu(UO_2)_2(PO_4)_2{\cdot}12H_2O$	$Cu_{0.9}(UO_2)_2(PO_4)_{1.8}$
Zeunerite	$Cu(UO_2)_2(AsO_4)_2{\cdot}12H_2O$	$Cu_{0.9}(UO_2)_2(PO_4)_{0.4}(AsO_4)_{1.5}$
Nováčekite	$Mg(UO_2)_2(AsO_4)_2{\cdot}12H_2O$	$Mg_{0.7}(UO_2)_2(PO_4)_{0.3}(AsO_4)_{1.2}$
Phosphuranylite	$Ca(UO_2)_3(PO_4)_2(OH)_2{\cdot}6H_2O$	$K_{0.7}Ca_{1.3}(UO_2)_3(PO_4)_{1.9}$
Andersonite	$Na_2Ca(UO_2)(CO_3)_3{\cdot}6H_2O$	$NaCa_3(UO_2)(SO_4)_{1.3}F_{1.7}$
Schröckingerite	$NaCa_3(UO_2)(CO_3)_3(SO_4)F{\cdot}10H_2O$	$Na_{0.5}Ca_{2.8}(UO_2)(SO_4)_{0.8}$
Johannite	$Cu(UO_2)_2(OH)_2(SO_4)_2{\cdot}8H_2O$	$Cu_{1.4}(UO_2)_2(SO_4)_{1.8}$
Natrozippeite	$Na_5(UO_2)_8(SO_4)_4O_5,(OH)_3{\cdot}8H_2O$	$Na_{2.5}(UO_2)_6(SO_4)_{2.7}$
Uranophane	$Ca(UO_2)_2(SiO_4)_2{\cdot}5H_2O$	$Ca_{0.8}(UO_2)_2(SiO_4)_{2.1}$
Kasolite	$Pb(UO_2)(SiO_4){\cdot}2H_2O$	$Pb(UO_2)(SiO_4$
Cuprosklodowskite	$Cu(UO_2)_2(SiO_4)_2{\cdot}6H_2O$	$Cu_{0.7}(UO_2)_2(SiO_4)_{2.5}$
Compreignacite	$K_2(UO_2)_6O_4(OH)_6{\cdot}7H_2O$	$K_{1.2}(UO_2)_6$

References

1 N. J. Elton and J. J. Hooper. Andersonite and schrockingerite from geevor mine, cornwall: two species new to britain. *Mineralogical Notes*, page 124, 1999.

2 R. L. Frost. An infrared and raman spectroscopic study of the uranyl micas. *Spectrochimica Acta, Part A*, 60:1469, 2004.

3 R. L. Frost, O. Carmody, K. L. Erickson, M. L. Weier, and J. Cejka. Molecular structure of the uranyl mineral andersonite - a raman spectroscopic study. *Journal of Molecular Structure*, 703:47 – 53, 2004.

4 R. L. Frost, J. Cejka, and G. Ayoko. Raman spectroscopic study of the uranyl phosphate minerals phosphuranylite and yingjiangite. *Journal of Raman Spectroscopy*, 39:495, 2008.

5 R. L. Frost, J. Cejka, G. Ayoko, and M. L. Weier. Raman spectroscopic and sem analysis of sodium-zippeite. *Journal of Raman Spectroscopy*, 38:1311, 2007.

6 R. L. Frost, J. Cejka, G. A. Ayoko, and M. J. Dickfos. Raman spectroscopic study of the multi-anion mineral schrockingerite. *Journal of Raman Spectroscopy*, 38:1609, 2007.

7 R. L. Frost, J. Cejka, M. L. Weier, and W. Martens. Molecular structure of the uranyl silicates - a raman spectroscopic study. *Journal of Raman Spectroscopy*, 37:538, 2006.

8 R. L. Frost, M. J. Dickfos, and J. Cejka. Raman spectroscopic study of the uranyl mineral compreignacite. *Journal of Raman Spectroscopy*, 39:1158, 2008.

9 R. L. Frost, K. L. Erickson, J. Cejka, and B. J. Reddy. A raman spectroscopic study of the uranyl sulphate mineral johannite. *Spectrochimica Acta, Part A*, 61:2702, 2005.

10 R. L. Frost and M. L. Weier. Hot-stage raman spectroscopic study of the thermal decomposition of saleeite. *Journal of Raman Spectroscopy*, 35:299, 2004.

11 R. L. Frost, M. L. Weier, and M. O. Adebajo. Thermal decomposition of metazeunerite - a high resolution thermogravimetric and hot-stage raman spectroscopic study. *Thermochimica Acta*, 419:119, 2004.